A NEW APPROACH TO GPS PHASE MULTIPATH MITIGATION

David Bétaille - *LCPC France / University College London*
Jon Maenpa, Hans-Jürgen Euler - *Leica Geosystems*
Paul Cross - *University College London - UK*

BIOGRAPHY

David Bétaille is a junior researcher at the LCPC (Laboratoire Central des Ponts et Chaussées - the French public works research institute) and belongs to the Site Robotics and Positioning subdivision. He has been involved in vehicle location using DGPS and dead reckoning for several years, supervising last year the development of an industrial prototype based on his design. David Bétaille is currently undertaking a PhD research program at University College London investigating phase multipath in kinematic GPS (a subject closely connected with precise positioning of machines for road construction and maintenance).

Jon Maenpa is Director of GPS Sensor Technology for the Corporate Technology Center of Leica Geosystems in Torrance, California, where he has worked since 1995. Prior to Leica, Jon was with Magnavox Advanced Products and Systems Company, where he worked on development of a variety of satellite navigation and satellite communication products since 1977. Jon holds a Bachelor of Science degree in Electrical Engineering from the University of California at Los Angeles, and he completed a graduate program at the Anderson School of Business, also at UCLA. Jon has authored numerous papers in the fields of satellite and radio navigation.

Hans-Jürgen Euler is Research Fellow at the Corporate Technology Center of Leica Geosystems AG in Heerbrugg, Switzerland. There he heads the Competence Team Positioning and Navigation researching algorithms for various applications. Hans-Jürgen received a PhD from the Technical University of Darmstadt in 1990 for his research in GPS ambiguity resolution. After working in Columbus, OH and Munich, Germany he joined 10 years ago Leica Geosystems in Heerbrugg. His main research interest are in the data-processing of GNSS observations and the combination with other sensors for precise positioning.

Paul Cross is Leica Professor of Geomatic Engineering at University College London (UCL), a post he has held for the last five years. He obtained his PhD from the University of Nottingham in 1970 and before joining UCL held teaching and research positions at the Universities of Nairobi, East London, Stuttgart and Newcastle. His main research interest is in precise GPS positioning and he currently concentrates on engineering and geophysical applications.

ABSTRACT

There have been a number of important developments in recent years in the mitigation of code multipath in GPS receivers but very little progress has been made with the mitigation of phase multipath and it remains the single-most important source of error in short baseline kinematic GPS and in most network Real-Time Kinematic (RTK) applications. University College London (UCL), the Laboratoire Central des Ponts et Chaussées (LCPC) and Leica Geosystems are collaborating in the development of methodologies to reduce this error source and so improve RTK GPS performance.

For several years Leica Geosystems have been developing a new GPS phase multipath mitigation technique leading to the ability of a receiver to deliver additional information from a separate dedicated correlator that enables the direct correction of the multipath-biased phase output from the measurement correlator. The technique has the potential to eliminate many multipath components and is based on sampling the received signals together with their possible multipath components before and immediately after code transitions. This paper explains the basic theory behind the method and summarises the key elements of the associated patents.

Two Leica System 500 receivers have been modified to incorporate the firmware necessary to use this new technique and a number of tests have been carried out to assess its capabilities both with lightweight and choke-ring antennas. These tests have been carried out at the LCPC near Nantes in France in May and June 2002. In order to create large multipath signals for some of the tests a 5 m by 2.5 m steel panel has been constructed and placed at different locations near to one of the antennas. Kinematic tests were carried out using the SESSYL kinematic positioning test bed, which consists of a carriage that can be moved in a controlled manner on an 180 m oval-shaped monorail. This enabled the roving antenna to be moved on a known trajectory in order to provide millimetre-level reference positions for the tests.

Initial results from the tests are extremely encouraging and are described in detail in this paper. The size of the multipath component of double differenced phase measurements has been reduced by up to 30% when using lightweight antennas and some of the theoretical characteristics of the method have been confirmed. The method is shown to have significant potential for reducing multipath at both roving receivers and at reference receiver locations, especially in cities and on engineering sites where high levels of multipath can often occur and where the number of satellites in view is critical.

INTRODUCTION

The dominant error source in the use of phase GPS for almost all kinematic applications, especially in civil engineering and robotics, is multipath. Multipath occurs when a direct signal from a satellite is mixed with one that has been reflected from one or more surfaces and can, in theory, cause errors of up to a quarter of a carrier signal wavelength in a measured range (i.e. 4.7 cm). It can occur at both reference antennas and at the roving antenna, making studies of GPS phase multipath in both static and kinematic modes important. Typically multipath induces errors of up to 1 cm and 2 cm respectively in horizontal and vertical kinematic positioning (although in some highly reflective environments these numbers can be larger, especially if the satellite geometry is poor) and it can seriously limit the use of GPS in some applications. For instance GPS is not sufficiently accurate to control pavement laying. Driving down multipath errors is probably the single-most important objective of current research into the use of GPS for engineering applications, as it is for attitude determination from GPS.

This paper introduces and tests a new technique for GPS phase multipath mitigation. It is based on the use of additional information from a separate dedicated phase correlator that enables the direct correction of the multipath-biased phase output from the normal measurement correlator. In the substantive part of this paper, we summarise the contents of various patents, particularly [STANSELL et al., 2000], on which the new correlator is based. These patents contain both a technique for code tracking, which is quite similar to that usually called "reference waveform" or "gated correlator" [McGRAW and BRAASCH, 1999], and an extension of this technique to phase tracking. This extension again relies on the gated correlator technique, called Multipath Mitigation Window (MMW) by its inventors, and throughout this paper.

After a brief review of the classical technique for phase tracking, a description of the phase MMW technique is given. This is followed by a presentation of the results of tests that were carried out using two modified Leica System 500 receivers at the LCPC, France, with the help of the SESSYL test facility. These test were carried out in both static and kinematic environments.

1. The classical technique of phase tracking

1.1. Phasor diagram

A phasor diagram, as in Fig. 1, is a 2-dimensional diagram in which the vertical axis corresponds to the value of the punctual in-phase product (I) and the horizontal axis corresponds to the value of the punctual in-quadrature product (Q). The products mentioned here are those of the received GPS signal with the generated replicas in the application specific integrated circuits (ASICs).

Suppose, for simplicity, that the received signal is:

signal = A(t) * db(t) * c(t) * sin(wt)　　　　　(1)

where A(t) is the amplitude of the received signal, db(t) the message data bit time series, c(t) the pseudo-random code time series. Note that both db(t) and c(t) modulate the phase of carrier wave sin(wt).

The replicas are:

IP = c(t+τ) * sin(wt+Φ), in-phase　　　　　(2a)
QP = c(t+τ) * cos(wt+Φ), in-quadrature　　　　　(2b)

where τ is the code synchronisation error of the replica with respect to the received signal, and Φ the phase synchronisation error.

I(t) = signal * IP　　　　　(3a)
　=A(t) * db(t) * c(t) * sin(wt) * code(t+τ) * sin(wt+Φ)
　= A(t) * db(t) * (cos(Φ)-cos(2wt+Φ))/2 * c(t+τ) * c(t)
Q(t) = signal * QP　　　　　(3b)
　=A(t) * db(t) * c(t) * sin(wt) * code(t+τ) * cos(wt+Φ)
　= A(t) * db(t) * (sin(2wt+Φ)-sin(Φ))/2 * c(t+τ) * c(t)

In fact, all these equations are not continuous in time, as the GPS received signal is sampled at discrete points, typically with a frequency of say approximately 40 MHz before entering the ASIC. Similarly, the replica is generated in a numerical form. In Leica geodetic receivers the exact sampling frequency is 4 * 10.23 MHz.

1.2. Predetection integration period

I and Q are not displayed in a phasor diagram as instantaneous values, but their averaged values are used. A vector in the phasor diagram represents I and Q integrated over a certain period, denoted as the 'integration period' or the 'predetection integration time' (PIT). For the phase measurement process the integration period is typically of the order of few ms, for instance 5 ms is used in Leica receivers.
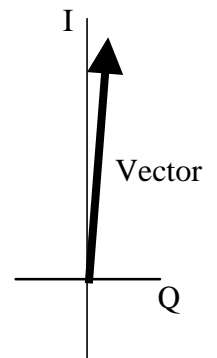

Fig.1. Phasor diagram

Such a period of time includes a very high number of carrier wave cycles, and causes the carrier wave terms cos(2wt) and sin(2wt) to be suppressed in the mathematical expressions of I and Q, since their averaged value is zero. 'db' denotes the value of the data bit, that remains constant during the PIT.

I = ∫$_{PIT}$ I(t)dt = db/2 * cos(Φ) * R(τ)　　　　　(4a)
Q = ∫$_{PIT}$ Q(t)dt = - db/2 * sin(Φ) * R(τ)　　　　　(4b)

Because of the relatively long duration of the integration period with respect to the period of the sampled GPS signal, I and Q are independent of the carrier wave. They only depend on

- the data bit ('db') that may alternate every 20 ms. It causes the vector in the phasor diagram flip to its opposite and reciprocally,

- the cross correlation of the code of the received signal and its replica ('R(τ)') computed over the 5 ms duration of the integration period. Hence, the amplitude of the vector in the phasor diagram may vary with code tracking in the code loop. When the code tracking is perfect, this amplitude equals 1, and

- the phase difference "Φ" between the received signal and its replica. This difference has a variation in time that depends on the frequency change of the NCO (Numerically Controlled Oscillator) with the temperature. Moreover, and particularly for high dynamics applications, the variation of Φ mainly depends on the change in the Doppler due to the kinematics of the satellite and the rover.

The maximum integration period of I and Q in a phase loop is related to the duration of the GPS message data bit, and is 20 ms. Actually, if the values of I and Q were averaged over more than 20 ms, it would mix the original vector in the phasor diagram and its opposite with an a priori unknown distribution in time and it would be impossible to make a decision with respect to driving the phase tracking loop. This is the way in which the GPS message is demodulated in the phase loop.

Lastly, we will recall the balance to be found between

- on the one hand, the interest in increasing the integration period, to make the measurement less sensitive to noise, and on the other hand,

- the interest in decreasing the integration period, to permit tracking when the rover receiver is subjected to high dynamics.

A predetection integration time of 5 ms is adequate to feed the phase loop as this usually has a bandwidth of around 20 Hz. This is because raw measurements in the correlator should be made at a frequency 10 times the bandwidth of the corresponding loop. Note that a 20 Hz bandwidth phase loop permits an output of 20 Hz independent phase data.

Moreover, within the 5 ms duration of the integration period, the phase difference between the received signal and its replica does not vary by more than about 1 degree. This can be demonstrated by computing the variation of the Doppler in time for a rover with an acceleration of 3 g, which is the maximum acceptable acceleration of the rover with a 20 Hz bandwidth 2nd order phase loop.

1.3. Discrimination function

The discrimination function used in a standard phase loop is:

$$DF = sign(I) * arctan(Q/I) \qquad (5)$$

or, more simply:

$$DF \sim sign(I) * Q \text{ since } |Q| << |I| \text{ and } |I| \sim 1. \qquad (6)$$

Both I and Q signals enable phase tracking despite the data bit alternation. Q is kept to 0 by the tracking loop, while I is maximum. Both I and Q are inversed at a data bit alternation. I changing to -I at a data bit alternation is detectable since $I >> 0$. The data bit polarity (and consequently the message data bit time series itself) is then determined and output. Furthermore, this data bit determination enables the driving of Q to 0 in the right way with the help of the NCO.

2. The standard phase loop functioning in the presence of multipath

Firstly, we examine the way in which a standard phase loop would work in a situation where a reflected signal is superimposed on the direct one.

Fig. 2 shows a portion of a direct signal with a single code transition and the same code transition, delayed, for a reflected signal. Note that in the figure the phase shift between the direct and the reflected signals exactly corresponds to the additional distance travelled by the reflected signal divided by the wavelength. In practice this might not be the case as the phase of the reflected signal is also shifted by up to +/- 180 degrees from that of the direct signal, depending on the physical properties of the reflector.

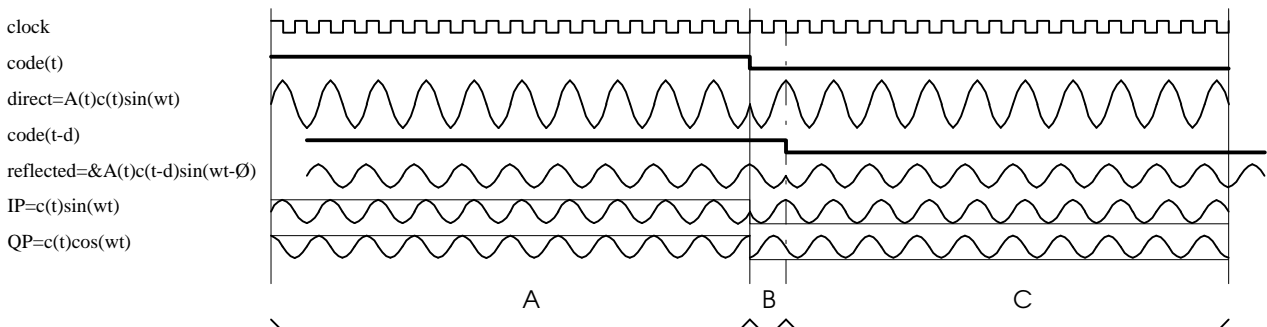Note: the time intervals A, B and C are explained further.

| clock |
| code(t) |
| direct=A(t)c(t)sin(wt) |
| code(t-d) |
| reflected=&A(t)c(t-d)sin(wt-Ø) |
| IP=c(t)sin(wt) |
| QP=c(t)cos(wt) |

A   B   C

Fig.2. Direct and multipath signals entering the standard phase loop

Let us now switch to the phasor diagram representation of the signals. We recall that the vertical axis is the 'I' product (product of the signal with a code prompt replica in phase: IP) and the horizontal axis is the 'Q' product (product of the signal with a code prompt replica in quadrature: QP).

The tracking loop is driven by the average of the I and Q values in time. The different components corresponding to the different signals that are present (direct and reflected) are added. The resulting vector is that entering the loop. The loop is closed so that the Q component of the resulting vector equals zero.

Fig. 3 shows the vectors A, B and C corresponding to the time interval A, B and C in Fig. 2:

- A is an interval before a direct code transition;

A = D+M, with D for direct component and M for multipath component.

- B in just after A and before the multipath code transition;

B = D–M. Compared to the first interval, M has changed to –M, since the polarity of the replica has changed (along with that of the direct signal), whilst the polarity of the reflected signal remains unchanged.

- C is just after B until the next direct code transition.

C = D+M = A. Compared to the second interval, –M has changed to M. The polarity of the reflected signal has changed, and it is now the same as that of the replica.
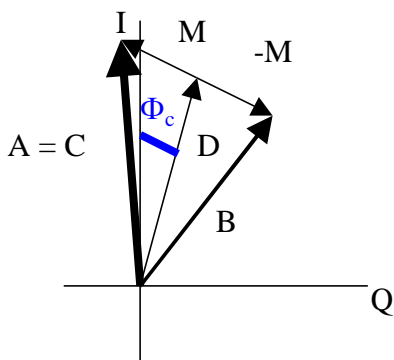
Fig.3. Phasor diagram of direct and multipath signals corresponding to the standard phase loop correlator

The standard phase loop averages continuously in time, which corresponds here (on the 2 chips duration of our example) to the summation of:

- A (during the first 40 samples);

- then B (during the next 3 samples);

- and finally A again, since C is equal to A (during the last 37 samples).

The ratio 3/(40+37) we have on the example given in the preceding figures keeps the same when integrating over the PIT, and it explains why the vector A and the vertical I axis corresponding to the tracking loop closure are not aligned. The I axis is slightly biased away from vector A toward vector B. The misalignment has the same proportion as the ratio of intervals A and B when integrating over time.

Moreover, the I axis is quite far from the vector D, which corresponds to the direct signal only. The alignment of the tracking loop onto the vector D would in fact produce the desired phase measurement, multipath free.

To conclude, the standard phase loop shows a bias (Φc) in case of multipath. It can also be shown graphically that the more the code is delayed, the less the tracking loop will be biased. It will be completely unbiased if the code is delayed by 1 chip or more.

3. The phase MMW correlator

As has been mentioned in the introduction, the MMW correlator has been introduced through a number of patents, e.g. [STANSELL et al., 2000]. It is essentially a phase MMW sampler that has a short polarized component before the direct signal code transition and followed by another short opposite component. This second component immediately follows the direct signal code transition, but ends before the multipath signal code transition. The polarity of these components is determined by the polarity of the code at the same time, exactly in the same way as in a standard phase loop.

Now, let us modify Fig. 2 as suggested by the patents. In Fig. 4, the polarity of the different components is positive and then negative due to the fact that the code transition is locally positive to negative.
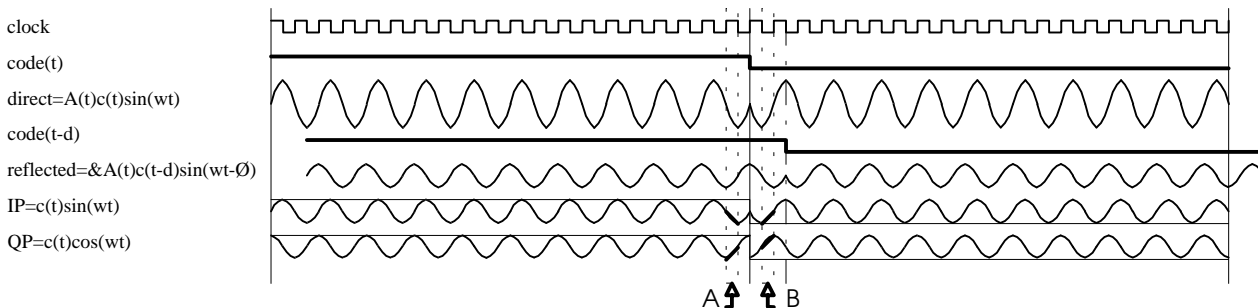

Fig.4. Direct and multipath signals entering the MMW phase loop

Using a phasor diagram representation, we show the vectors A and B, which are respectively the composite vectors corresponding to the first and second intervals of the MMW sampler. A = D+M, and B = D−M. There is no interval C.
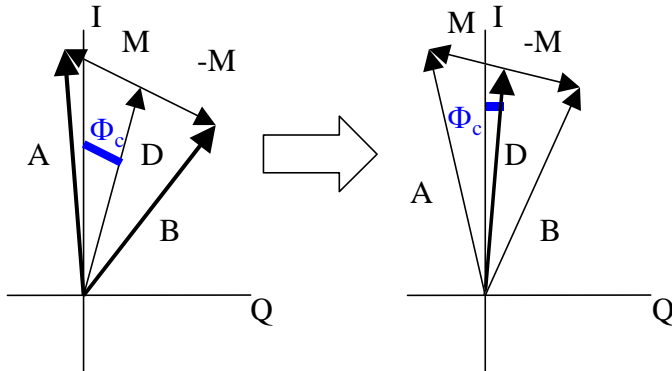

Fig.5. Phasor diagram of direct and multipath signals corresponding to the MMW phase loop correlator

The invention relies on the key observation from Fig. 3 that the vector average of vectors A and B is vector D, which corresponds to the direct signal without any multipath distortion. If vectors A and B have the same 'weight' in the integration carried out by the tracking loop, then the tracking loop will be aligned on vector D (Φc, the multipath phase error, becomes zero).

Therefore, instead of integrating continuously as in a standard phase loop, the MMW technique integrates only during the MMW samples. The technique is neither limited by the number of reflected signals nor by their amplitude.

4. Implementation issues

4.1. Received signal bandwidth

The MMW correlator works provided that the occurrence of the multipath signal transitions are sufficiently delayed with respect to the direct code transitions, for the measurement samples to be taken. In other words, the sooner a sample is taken in the received signal after a code transition, the better.

Hence, the bandwidth of the received signal that enters the phase loop is of great importance. This bandwidth is around 25 MHz, which means that a code transition will last for some 40 ns. Consequently, an equivalent delay must occur before taking a sample in the received signal. With a clock rate of 40 MHz, the first sample comes after a delay of 25 ns by which time the code transition is not quite complete. It is, however, considered to be just sufficient with regard to the bandwidth of the signal.

40 MHz (which corresponds to an additional path length of approximately 7.5 m) is therefore a good trade-off between the duration of the code transition and the capability of the MMW to mitigate multipath. Increasing this rate would enable multipath with shorter delays (i.e. from closer reflectors) to be mitigated but would lead to an increase in noise due to use of a less complete code transition.

Consequently in Leica's current implementation of the MMW, only reflected signals with an additional path length over 7.5 m will be theoretically eliminated in total, while reflected signals with shorter path lengths will be mitigated to a lesser extent.

4.2. Signal to noise ratio

Compared to a standard phase loop, the signal content is divided by 40 (1 sample instead of 40 per code chip). As a consequence, the signal to noise ratio (SNR) is reduced by $10 * \log_{10}(1/40)$ (i.e. 16 dB).

In practice, it is impossible to drive the phase loop with I and Q outputs from the MMW correlator because of its high sensitivity to noise. The solution adopted in Leica's implementation is to keep the phase tracking process unchanged by integrating I and Q in the standard loop at the usual periods of respectively 20 ms and 5 ms. The MMW correlator operates in parallel and outputs I_{MMW} and Q_{MMW} with its original sampling of 1 per 40 clock samples, but with a much larger integration period, in order to improve the SNR. A one second integration period was employed for this test series. Of course this leads to time correlation in the output values of I_{MMW} and Q_{MMW}, which might be noticeable in high kinematic applications.

Thus, the phase measurements remain biased in the presence of multipath, but the additional observables I_{MMW} and Q_{MMW} output by the MMW correlator enable the correction of this bias. The phase multipath error Φc is simply given by:

$$\Phi c = \arctan(Q_{MMW}/I_{MMW}) \qquad (7)$$

which can be directly applied to the measured phase.

5. Tests programme

The equipment that was used in the tests comprised two pairs of Leica GPS L1/L2 antennas (2 lightweight AT502 and 2 choke-ring AT504 antennas) and a pair of Leica SR530 L1/L2 receivers.

The receiver firmware was modified to permit logging at 1 Hz of both standard phase measurements and the I and Q outputs of the phase MMW correlator. As explained before, these outputs enable the computation of the phase corrections ($\arctan(Q_{MMW}/I_{MMW})$) to be applied to the standard phase measurements epoch by epoch.

For the static tests, both base and rover antennas were set on tripods in the grass field surrounding the SESSYL tests bed. The rover was placed on the SESSYL carriage for the kinematic tests. In both cases the baseline length was less than 100 m. The kinematic tests were carried out at 0.1 m/s constant speed, along a 50 m straight section of the SESSYL track (see Fig 10).

The baseline, both in the static and kinematic cases, was known in 3 dimensions with an accuracy of 1 mm (1 σ). SESSYL reference data were time tagged by GPS PPS acquisition.

A 5 m x 2.5 m metal reflector was specially constructed to support the tests. It was fixed to the side of

a van parked in the vicinity of the rover station (middle of the 50 m straight for SESSYL tests). The reflector was always placed north the antenna, ~ 30° tilted (in order to avoid reflection coming from low elevation satellites), at a distance of 2 m or 5 m from the antenna, with the centre of antenna near the middle of the reflector.
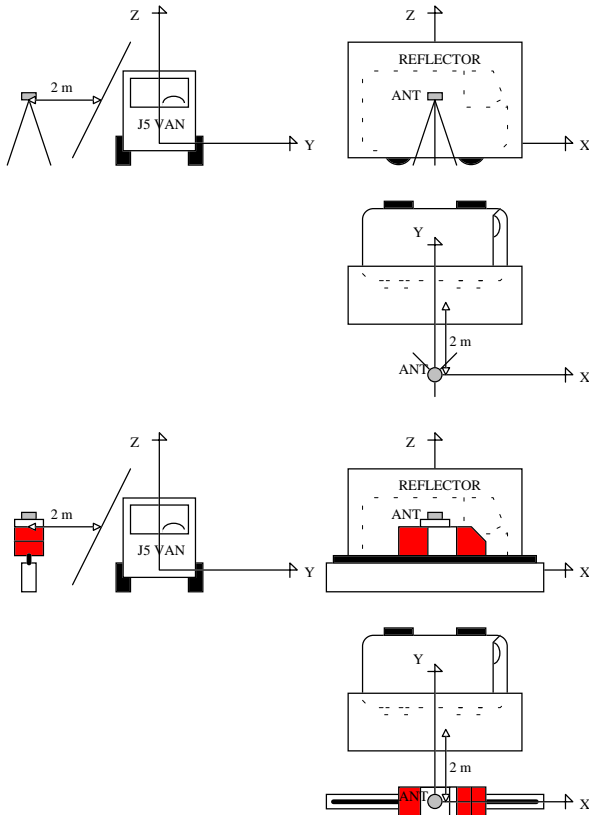

Fig.6. Setup of the reflector near the rover antenna

A total station was used to determine the position of the reflector in the local reference frame with the same accuracy as the antennas, i.e. 1 mm (1 σ).

The kinematic tests with SESSYL started at the same sidereal time each day, in order to keep the same constellation at the antenna locations an so maintain identical geometry between the tests. A summary of these and the static tests is given below.

	Week 1: static	Week 2: kinematic
No reflector	Lightweight	Lightweight
Reflector at 5 m	Lightweight	Lightweight
Reflector at 5 m	Choke Ring	Choke Ring
No reflector	Choke Ring	Choke Ring
Reflector at 2 m	Choke Ring	Lightweight

In the following results, we selected several satellites, whose position relative to the reflector and the rover antenna caused severe multipath, for detailed analysis. Time series of Observed-Computed (O-C) Double Differences (DD) of L1 phase measurements are displayed. The Computed DD rely on the known position of the rover. Note that the differencing satellite was always too high to be affected by multipath on the panel.

In all cases time series are duplicated, with and without applying the corrections of L1 phase measurements provided by the MMW phase correlator.

6. Results of static tests

6.1. Lightweight antenna; reflector at 5 m

The O-C L1 phase DD errors resulting from the tests with the lightweight antenna are given in Fig. 7a. SV2 has been selected. Multipath is clearly visible and the frequency, phase and amplitude of the resulting phase error correspond closely to those predicted by multipath modelling [GEORGIADOU and KLEUSBERG, 1987].

The periods of multipath occurrence (determined geometrically with the help of the precise reference positioning) are identified by a 'green' window superimposed onto the time series.
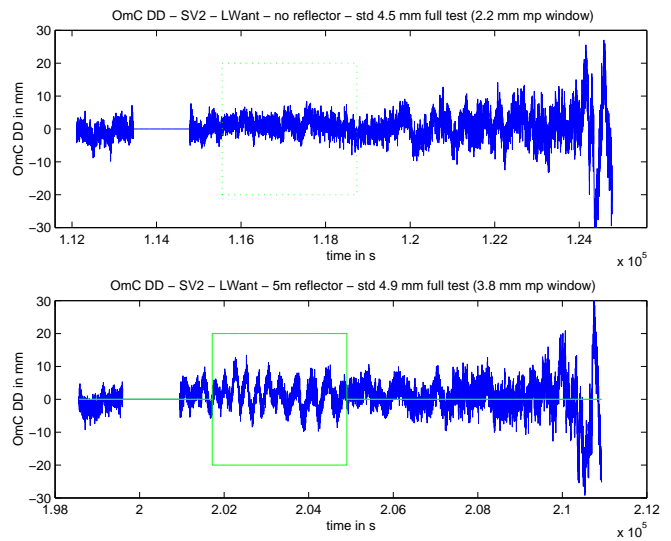
Fig.7a. Static lightweight antenna (at 5 m), no correction

Fig. 7b is the equivalent to Fig. 7a, but after application of the output from the MMW phase correlator, i.e. after correcting for phase multipath.
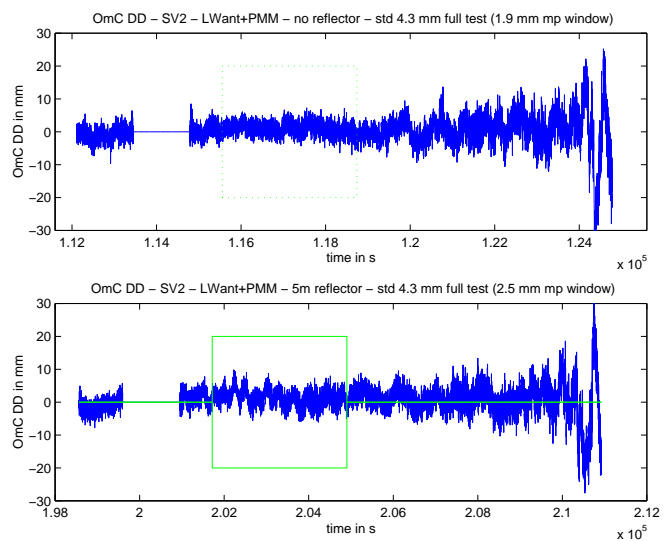

Fig.7b. Static lightweight antenna (at 5 m), MMW correction

The results are summarised below.

Lightweight antenna		Std dev (mm) PMMW off	Std dev (mm) PMMW on	Gain
Day 1	no reflector	2.2	1.9	14%
Day 2	reflector **5 m**	3.8	2.5	34%

Multipath is also clearly visible on the O-C L1 phase DD errors from the experiments with the choke ring antenna, see Fig. 8a, but its amplitude is significantly reduced compared with that for the lightweight antenna.
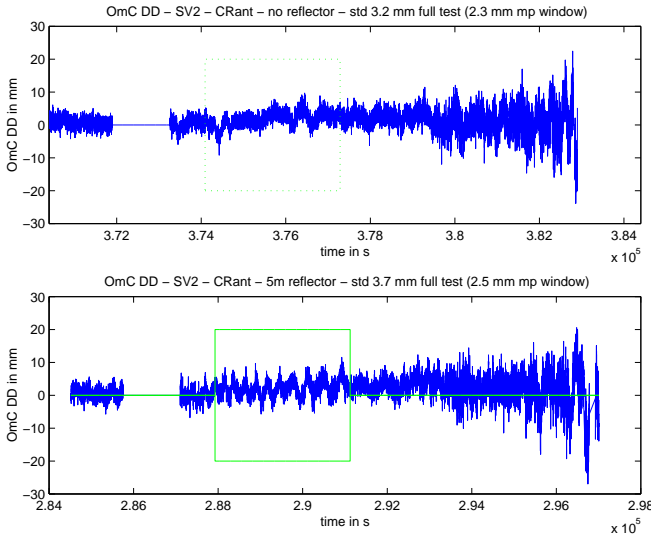

Fig.8a. Static choke ring antenna (at 5 m), no correction

It can be seen from Fig. 8b that when a choke ring antenna is used and corrections to the L1 phase measurements made using the phase MMW, it appears that the standard deviation of the phase error, despite multipath, equals that when no multipath exists.
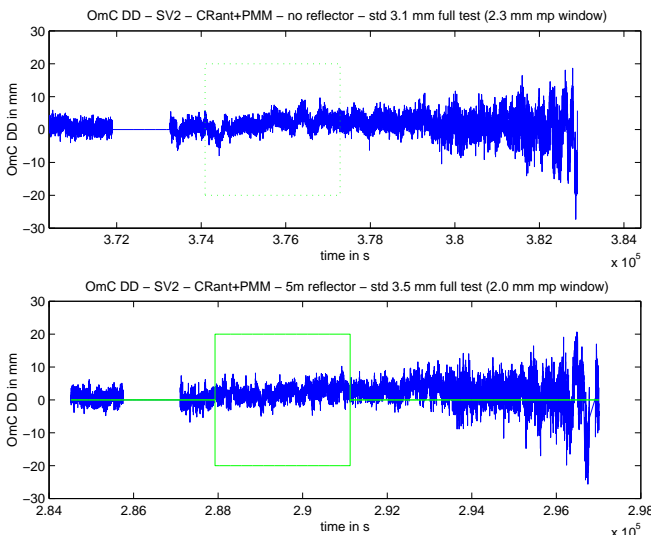
Fig.8b. Static choke ring antenna (at 5 m), MMW correction

The results are summarised below.

Choke ring antenna		Std dev (mm) PMMW off	Std dev (mm) PMMW on	Gain
Day 4	no reflector	2.3	2.3	0
Day 3	reflector **5 m**	2.5	2.0	20%

6.3. Choke ring antenna; reflector at 2 m

The same test as in §6.2 was repeated with the reflector placed at a distance of about 2 m from the antenna. The resulting time series are shown in Fig 9a. At this distance, the additional path length corresponding to the satellite observed here is between 2 m and 4 m (whereas it was between 6.5 m and 8.5 m with the reflector at 5 m).
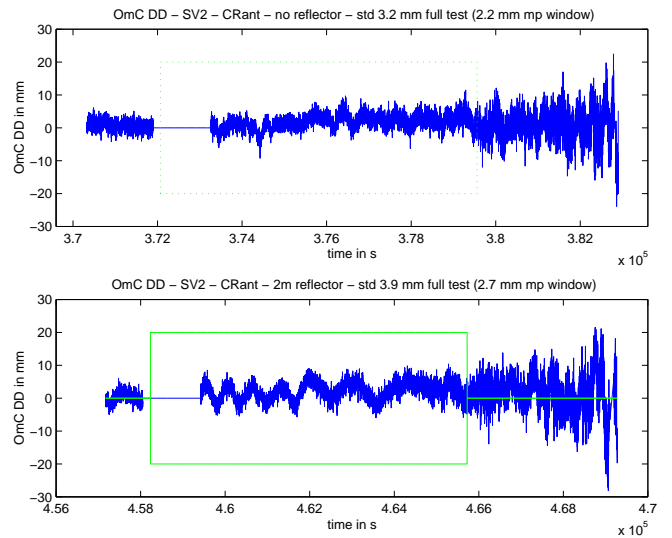
Fig.9a. Static choke ring antenna (at 2 m), no correction

As expected for this case, the phase MMW correlator is much less effective in mitigating the multipath error, due to the fact the additional path length is well under the 7.5 m point, as discussed in §4.1.
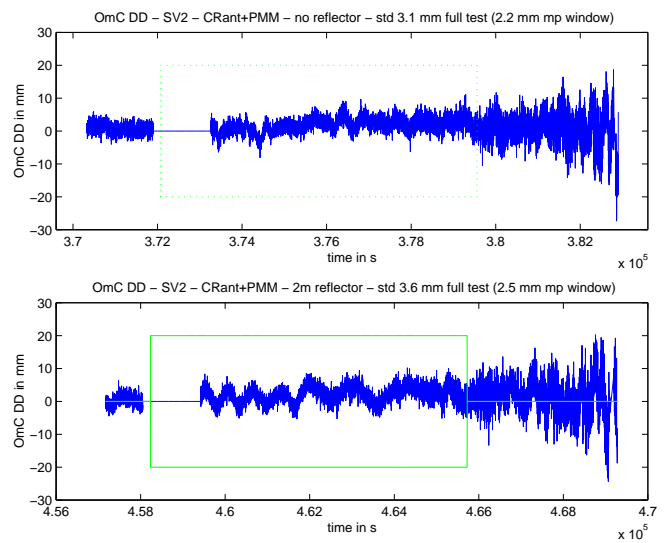
Fig.9b. Static choke ring antenna (at 5 m), MMW correction

The results are summarised below.

Choke ring antenna		Std dev (mm) PMMW off	Std dev (mm) PMMW on	Gain
Day 4	no reflector	2.3	2.3	0
Day 5	reflector **2 m**	2.7	2.5	7%

7. Results of kinematic tests

7.1. Lightweight antenna; reflector at 5 m

Three satellites (SV2, SV22 and SV31) exhibited significant (although not severe) multipath in the kinematic tests with the lightweight antenna passing the reflector at a distance 5 m, and were selected for detailed analysis. In each case, the duration of the theoretical multipath occurrence was around 100 s, which

corresponds to the time that SESSYL was in front of the 5 m long panel when travelling at 0.1 m/s, see Fig. 10.

The O-C L1 phase DD errors are given in Fig. 11a, in a similar format to the static tests, e.g. Fig. 7a. Note that the time scale of this figure is different from that of Fig. 7a and the other static tests (total period of ½ hour for kinematic tests compared with 4 hours for static tests).
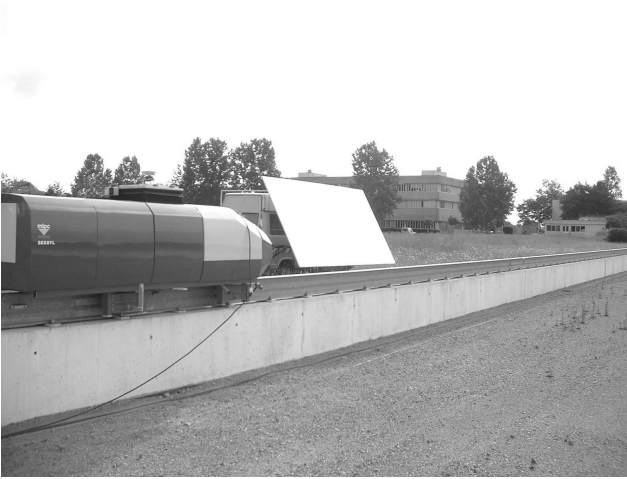

Fig.10. Photo of the SESSYL tests (light weight antenna)

The overall trend in the O-C L1 phase DD errors is due to multipath from the metallic 0.5 m square plate on top of SESSYL and on which the antenna is mounted at a height of 0.2 m. This additional source of multipath causes a phase error characterised by a much lower frequency than that caused by the panel. Within the ½ hour duration of each test, this trend can be approximated as being linear with time.

The statistics given on top of each of the figures are affected by this low frequency multipath error. However, the standard deviation, amplitude and maximum absolute error displayed within the frame of each figure were computed after modelling it as a linear trend, and then removing it. The trend itself is displayed in black. The maximum absolute error (denoted |ê| and given in the lower left corner of each frame) is computed after filtering the de-trended error values (with a 3 value median filter).

Special attention should be paid to the oscillating shape of the error within the green multipath window, i.e. when SESSYL passes in front of the steel plate (rather than examining the numerical statistics in too much detail). The application of the phase MMW correlator results in a clear global attenuation of the amplitude of the error within this window (see Fig. 11b).

The results are summarised below.

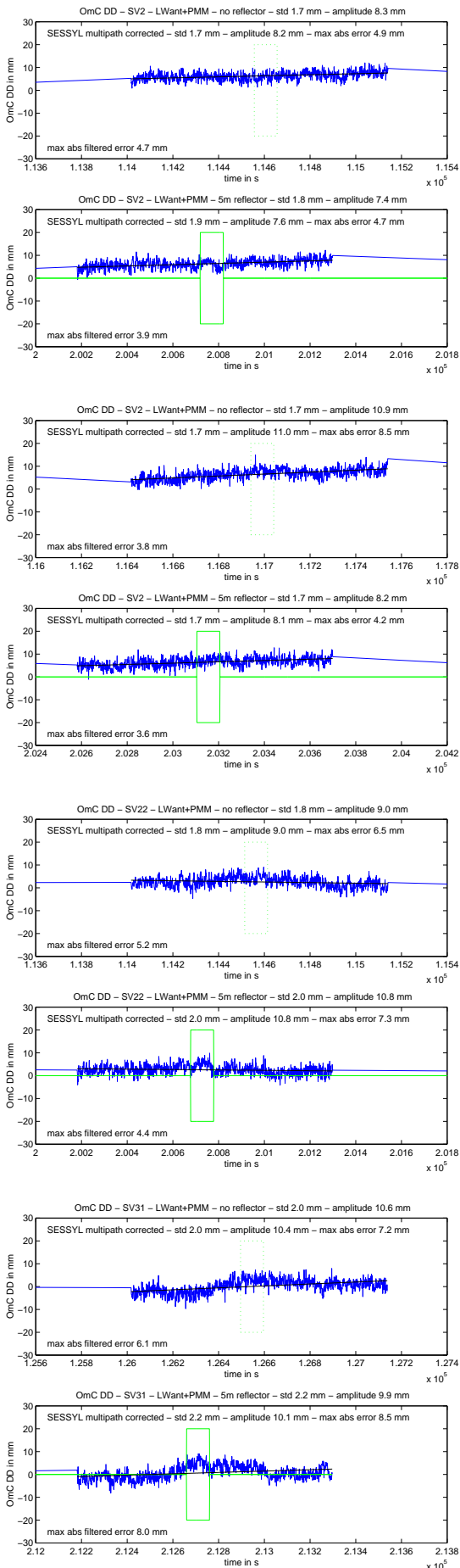| Lightweight antenna □day	Std dev (mm) and |ê| (test by test) PMMW off	Std dev (mm) and |ê| (test by test) PMMW on	Average gain
1 no reflector	1.7 / 1.8 / 1.9 / 2.0	1.7 / 1.7 / 1.8 / 2.0	3%
1 no reflector	4.8 / 3.8 / 5.6 / 6.3	4.7 / 3.8 / 5.2 / 6.1	3%
2 reflector **5 m**	2.2 / 2.1 / 2.7 / 2.4	1.9 / 1.7 / 2.0 / 2.2	17%
2 reflector **5 m**	3.7 / 4.7 / 7.3 / 11.1	3.9 / 3.6 / 4.4 / 8.0	21%
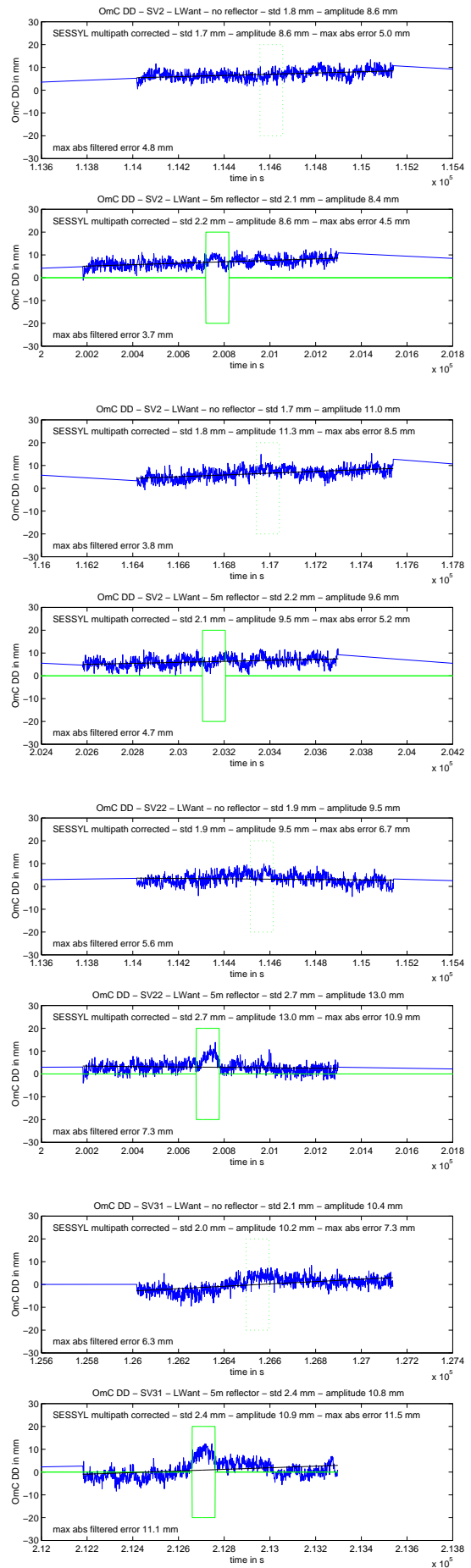
Fig.11a. Kinematic lightweight antenna (5 m), no correction

7.2. Choke ring antenna; reflector at 5 m

By visual inspection of the choke ring graphical results (not included here), we noticed that the low frequency error (caused by the SESSYL metallic plate) almost disappeared, as did the oscillating shape within the green windows (caused by the 5 m steel plate). In other words the multipath caused by both the panel and the SESSYL plate were very weak, i.e. they were efficiently attenuated by the choke ring antenna itself.

In this case the application of the phase MMW process, not surprisingly, made no noticeable difference to the results.

7.3. Lightweight antenna; reflector at 2 m

The time series and statistics for the results of the kinematic tests with the lightweight antenna passing the reflector at a distance of 2 m are shown in Figs. 12a and 12b have the same meanings as those described in §7.1 and Figs. 11a and 11b. The trend due to multipath from SESSYL has again been removed to compute the standard deviations and the maximum absolute filtered error ($|\hat{e}|$).

As was mentioned in §4.1, the additional path length (determined by the distance to the reflector) is a critical parameter with regard to the functioning of the phase MMW correlator. In the results of the kinematic tests at 2 m, it can be seen that, as expected and as in the case of the static trials, the MMW correlator is unable to mitigate appreciably the multipath error. This is because the additional path length is significantly less than 7.5 m. Nevertheless, the process does lead to a small improvement in the results, which are summarised below.

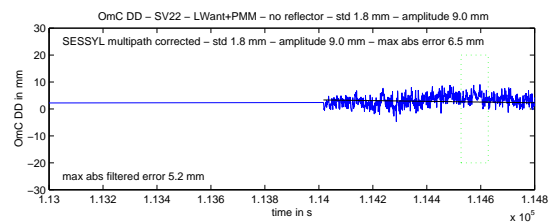| Lightweight antenna □day	Std dev (mm) and $|\hat{e}|$ (test by test) PMMW off	Std dev (mm) and $|\hat{e}|$ (test by test) PMMW on	Average gain
1 no reflector	1.8 / 1.8 / 1.9 / 1.9	1.8 / 1.7 / 1.8 / 2.0	1%
1 no reflector	4.8 / 3.8 / 5.6 / 6.3	4.7 / 3.8 / 5.2 / 6.1	3%
5 reflector **2 m**	2.3 / 4.3 / 4.0 / 3.3	2.3 / 4.0 / 3.0 / 2.5	14%
5 reflector **2 m**	5.1 / 6.7 / 8.2 / 7.2	5.2 / 5.9 / 6.2 / 5.8	13%

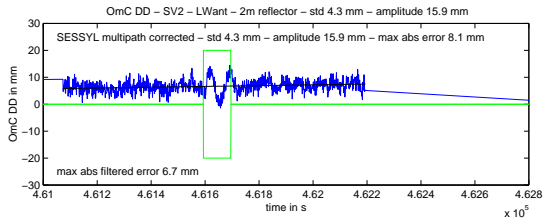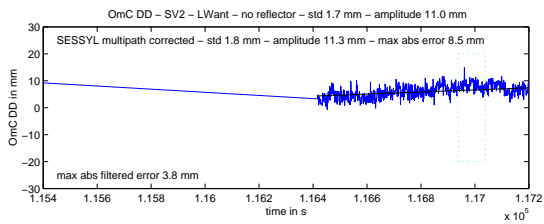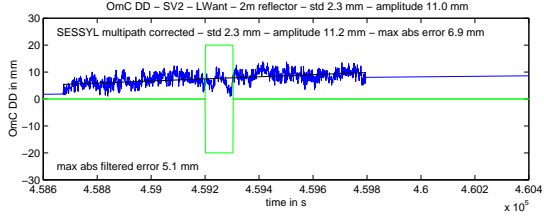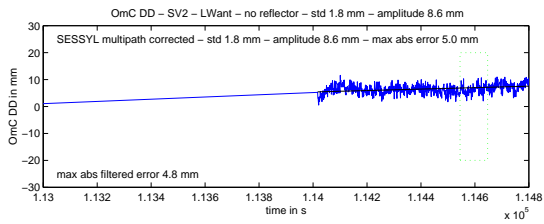*Fig.11b. Kinematic lightweight antenna (5 m), MMW correction*
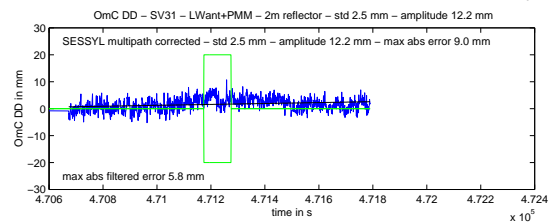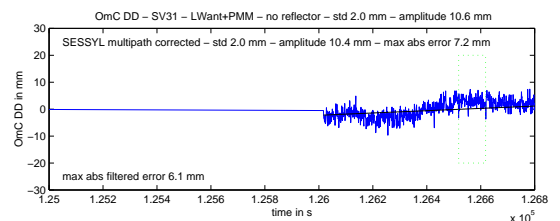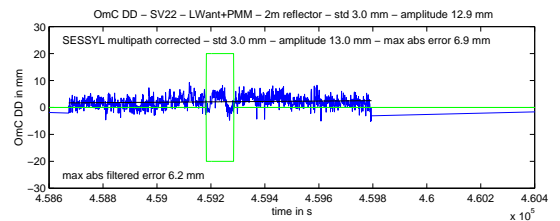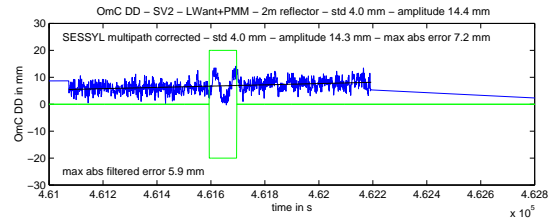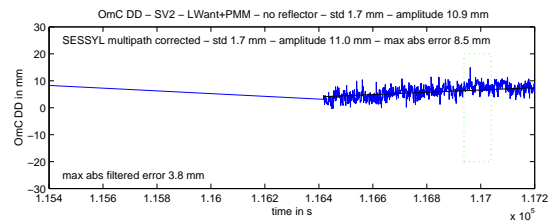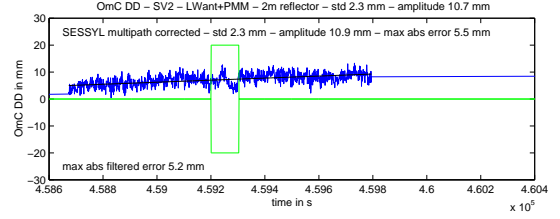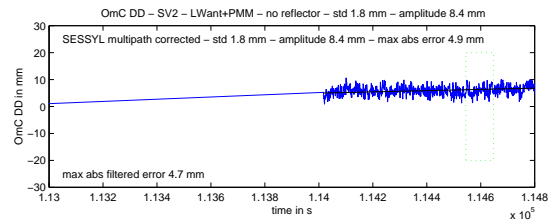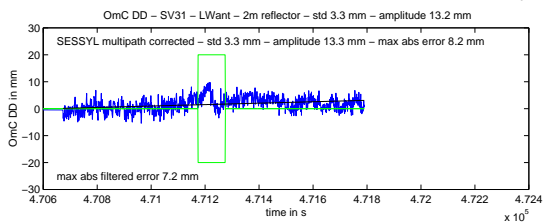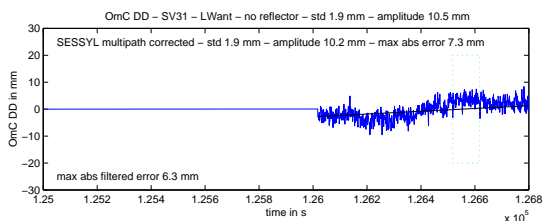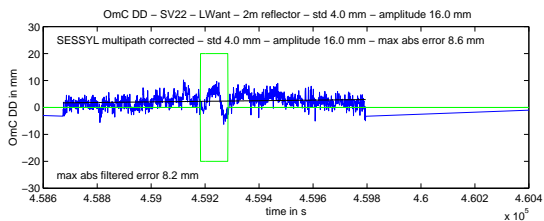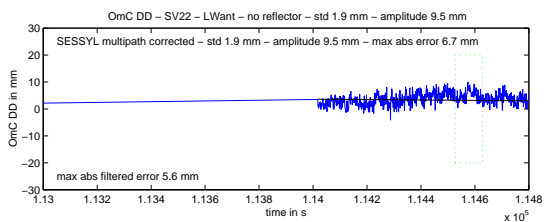
Fig.12a. Kinematic lightweight (5 m) antenna, no correction   *Fig.12b.* Kinematic lightweight antenna (2 m), MMW correction

CONCLUSIONS

The patented phase MMW technique enables the measurement of the phase of the direct signal by vector summing (integrating) the composite vector before every code transition with the composite vector immediately after such transitions (but before the arrival of the transitions on any reflected signals).

The campaign of tests carried out at the LCPC showed that this technique, as implemented in the Leica System 500 receiver, always improved GPS phase measurements. It did this by

- reducing the noise of the phase measurements – so leading to an improvement irrespective of the presence of the reflector (there is never a multipath free environment); and

- significantly reducing the impact of multipath as long as the additional path length of the reflected signal was at least 7.5 m.

In the static tests, the MMW correlator improved the multipath affected phase measurements by 34% (lightweight antenna tests) and 20% (choke ring antenna tests) with a reflector sufficiently far away (additional path length greater than 7.5 m).

The results of the kinematic tests are harder to interpret as the time periods of multipath occurrence are of a rather short duration. The results do, however, indicate that the application of the MMW correlator leads to significant improvements in the measurements. The incidence of the reflecting panel on the measurements was clearly visible when the lightweight antenna was used and the correlator improved the phase measurements by of the order of 20% (with a reflector sufficiently far away). For the choke ring antenna, we obtained sub-centimetre statistics irrespective of the presence of the reflecting panel and no clear multipath influence on measurements was noticed.

The fact that the mitigation was not effective for close-by reflectors was confirmed by the results of applying the MMW correlator when the panel was at a distance of only 2 m in both the static and kinematic tests. Also in the kinematic tests multipath from the SESSYL plate at a distance of 0.2 m was not mitigated. However, application of the results of the MMW correlator always improved the phase measurements (by up to 10%) due to a general noise reduction of the measurements.

REFERENCES

[GEORGIADOU and KLEUSBERG, 1987] – Georgiadou, Y., A. Kleusberg, On carrier signal multipath effects in relative GPS positioning, Manuscripta Geodaetica, Vol. 13, pp. 172-179, 1988

[HATCH et al., 1997] – Hatch, R.R., R.G. Keegan, T.A. Stansell, Leica's code and phase multipath mitigation techniques, a Leica's letter, Torrance, California, 1997

[HATCH, 2000] – Hatch, R.R., Method and apparatus for code synchronisation in a GPS receiver, US patent 6,163,567, 2000

[STANSELL et al., 1996] – Stansell, T.A., J.E. Knight, R.G. Keegan, R.R. Hatch, C.R. Cahn, Mitigation of multipath effects in GPS receivers, world patent WO 96/37789, 1996

[STANSELL et al., 2000] – Stansell, T.A., J.E. Knight, R.G. Keegan, C.R. Cahn, Mitigation of multipath effects in GPS receivers, US patent 6,160,841, 2000

[McGRAW and BRAASCH, 1999] – McGraw, G., M. Braasch, GNSS multipath mitigation using gated correlator technique, Proceedings of ION NTM-99, San Diego, California, pp., 1999